Nuclear Engineering and Technology 50 (2018) 1426–1432

Contents lists available at ScienceDirect

Nuclear Engineering and Technology

journal homepage: www.elsevier.com/locate/net

Technical Note

A scintillation detector configuration for pulse shape analysis

Phan Van Chuan [a], Nguyen Duc Hoa [a], Nguyen Xuan Hai [b, *], Nguyen Ngoc Anh [b], Nguyen Nhi Dien [b], Pham Dinh Khang [c]

[a] Dalat University, 01 Phu Dong Thien Vuong, Dalat, Viet Nam
[b] Dalat Nuclear Research Institute, 01 Nguyen Tu Luc, Dalat, Viet Nam
[c] Hanoi University of Science and Technology, 01 Dai Co Viet, Hanoi, Viet Nam

ARTICLE INFO

Article history:
Received 10 November 2017
Received in revised form
12 May 2018
Accepted 16 July 2018
Available online 18 July 2018

Keywords:
Neutron scintillation detector
Pulse shape discrimination
Neutron/gamma discrimination

ABSTRACT

This paper presents a neutron detector configuration using EJ-301 scintillation liquid, a R9420 photomultiplier and a homemade preamplifier. The detector qualities which include the energy linearity, efficiency response and neutron/gamma discrimination are guaranteed for neutron detection in the energy range from 0 to 3000 keVee. Regarding the neutron/gamma discrimination capability, four pulse shape discrimination (PSD) methods which are the threshold crossing time (TCT), pulse gradient analysis (PGA), charge comparison (CC) and correlation pattern recognition (CPR), were evaluated and discussed; among of these, the CPR method provides the best neutron/gamma discrimination.

1. Introduction

The EJ-301 liquid scintillator exhibits excellent PSD properties, particularly for fast neutron counting and spectrometry in the presence of gamma radiation [1–3]. This kind of scintillator could be used to detect both neutron and gamma-ray. Therefore, the neutron/gamma discrimination efficiency is the most important characteristic. It is well known that the neutron/gamma discrimination of detector depends on not only scintillator properties but also PSD methods.

Many PSD methods have been evaluated and reported, such as zero-crossing (ZC) [2,4–6], PGA [7], CC [2,4,5,7,8], frequency gradient analysis (FGA) [9], TCT [10], discrete Fourier transform (DFT) [11], CPR [12], etc. The CC and ZC methods are commonly implemented; therefore, they have become the industrial standards which are used to compare with new discrimination methods [4,9]. Figure-of-merits (FoM) factor is used for comparing method qualities.

For each method, FoM depends on device specification and analog or digital PSD technique [4]; in digital PSD method, resolution and rate of sampling process are one of those reasons. For example, when comparing the ZC and CC methods, the results in Refs. [5,6] were contrary to each other.

The advantage of digital technique was shown in Ref. [4], but in Ref. [5] the analog technique was excellent. Wan et al. have re-investigated CC and ZC methods [2], the results were agreed with Ref. [5], except that they investigated the comparison between CC and ZC methods using analog PSD technique. At the energy threshold of 80 keVee and lower, ZC method was better. At higher energy, CC method presented better separation [2].

Most studies used PMTs which have twelve dynodes; therefore, the results are somewhat limited to apply. In sampling process, the signals from PMTs which have less than twelve dynodes are of small amplitude and strongly distorted. In order to avoid the distortion of signals, the fast response time PMT and fast preamplifier are used to improve the signal-to-noise ratio before sampling. In addition, to minimize distortion in original neutron spectrum, the size of monitor detector has to be as small as possible [3,15].

The popular commercial preamplifiers [16,17] have a long tail pulse which is about 50 μs and needs to be connected to detector through the cables [14,18]. Because of these reasons, decay time specification of neutron-gamma pulse induces from scintillator liquid and signals transmitting through cable could be noised and distorted.

Nowadays, scintillator and fast amplifier integrated circuits (IC) are popularly available at low cost; therefore, it is easy to design and set up a neutron spectroscopy for specific applications.

This work focused on manufacturing of a special low-cost

* Corresponding author.
E-mail address: nxhainri@gmail.com (N.X. Hai).

https://doi.org/10.1016/j.net.2018.07.009

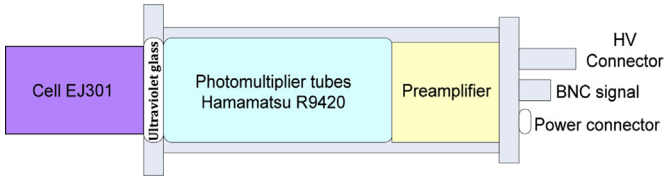

Fig. 1. Layout of neutron detector.

neutron detector but having high qualities for neutron monitoring and training purposes. At the same time, four PSD methods which are TCT, PGA, CC and CPR were re-investigated.

2. Experiment

2.1. Detector making

The layout of neutron detector in this work is shown as in Fig. 1, includes liquid scintillator container (cell), photo-multiplier tube (PMT), voltage divider, cover shield and preamplifier. The cell is left cylinder made of aluminum with 34-mm diameter and 60-mm length in size. The inner surface of the cell was polished, matched PMT through ultra violet (UV) glass window with 2-mm thickness. The PMT is Hamamatsu R9420; it has 1.6 ns rise and 550 ps spread time, respectively [19]. The anode of PMT is connected to preamplifier which is described in below section. The cell, PMT and the preamplifier are housed in cover shield which is cylindrical aluminum with 49-mm diameter and 200-mm length in size; that prevent light from outside and magnetic interference. The connectors of high voltage, signal and power supply are mounted at the tail of the detector.

2.2. Preamplifier making

The fast decay component of EJ-301 is about 3.2 ns [1], therefore, the signals which induced from PMT's anode have short rise-time (less than 5 ns). Besides, the pulse signals are distorted by transmission through cable to the digitized block [3]. So, the preamplifier is needed to generate appropriate pulse shapes and remove high frequency noise. To meet these demands, a preamplifier was designed for linear output voltages in the near above zero to 2.2 V, corresponding to the energy range from 0 to 3100 keVee. The preamplifier consists of four main stages: first is converts current to voltage pulses by the load resistance, second is voltage amplifier with gain of 30 times, next is filter by sallen-key low pass filters (f_{-3}dB = 33.8 MHz, butterworth = 0.6), and then is impedance matching (50Ω). The typical output pulse shapes are 12 ns rise time, 21 ns fall time and total gain of 17.85 times; that remains the output amplitude of the Compton edge of 662 keV and 1332 keV are 344.7 mV and 806.8 mV, respectively.

2.3. Testing

Preamplifier testing: a test setup is shown in Fig. 2. The instruments include 419 pulse generator, capacitor box and DPO7254C oscilloscope. All BNC connectors at the ends of cables are in good mechanical condition to assure low-resistance electrical connection. A back-terminating resistance of 50 Ω is assumed for the pulse generator and preamplifier under test, therefore, cables and connectors are compatible, and correctly terminated. The capacitor box is particular component with high accuracy and the errors are not greater than 1%. The generator signal was set at 5 ns rise time and 20 μs fall time; the parameters of capacitor box were adjusted to match the time constant of the PMT if it is longer than the time constant of the preamplifier. The pulse's amplitude at preamplifier input is changed by manual which is from 10 to 300 mV with 10 mV in per step. The output of capacitor box is connected to input of preamplifier, at the same time, both input and output of preamplifier are connected to first and second channels of oscilloscope, therefore, all signals changing were simultaneously analyzed. Oscilloscope is DPO7254C model, which was operated at 1 Giga sampling per second (GSPS) and 2.5 GHz bandwidth. In each changing of input, the values of amplitude and standard deviation of the pulses were analyzed. The measured preamplifier noise shall be corrected for the main-amplifier noise in the following way: after determining e_{no}, disconnect the preamplifier and terminate the input of the main amplifier with impedance that is the same as the output impedance of the preamplifier. Record the new (e'_{no}). The corrected noise due to preamplifier alone is the quadratic difference as equation (1) [20], and the results are shown as in Table 1.

Table 1
The specifications of preamplifier.

Parameters	Value
Measuring range	0 ÷ 3000 keVee
Total noise	797.9 ± 0.34 μV (equivalent of 1.13 keVee)
Baseline	35.8 ± 0.288 mV
Sensitivity[a]	~ 707 mV/MeV

[a] Amplitude pulse in mV per MeV of gamma-rays energy deposited in the scintillation cell of detector.

$$\left[(e_{no})^2 - (e'_{no})^2\right]^2 \quad (1)$$

Energy linearity: the detector's energy non-linearity depends on scintillation liquid and preamplifier, which can be evaluated through gamma-ray decay from radioisotope sources [1,3]. In this test, ^{22}Na (333 kBq 12/2000), ^{137}Cs (407 kBq 05/2011) and ^{60}Co (407 kBq 12/2000) sources were used to evaluate the energy linearity of the detector. In order to reject effects of amplifier, the detector was set up directly with DPO7254C oscilloscope that operated in modes of amplitude and spectrum measurement; the high voltage for detector was set at −1200 V and supplied by high voltage power block of Canberra 3002D model. Based on the measured spectrum, the relation between pulse height and gamma energy, which were defined by equation (2) [3].

$$E_c = E_\gamma \left(1 - \frac{1}{1 + \frac{2E_\gamma}{m_e c^2}}\right) \quad (2)$$

where E_c, E_γ, m_e and c are maximum back-scatter energy,

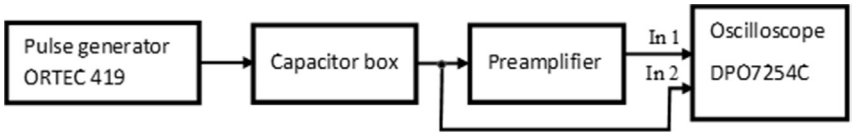

Fig. 2. The configuration of linearity evaluation for preamplifier.

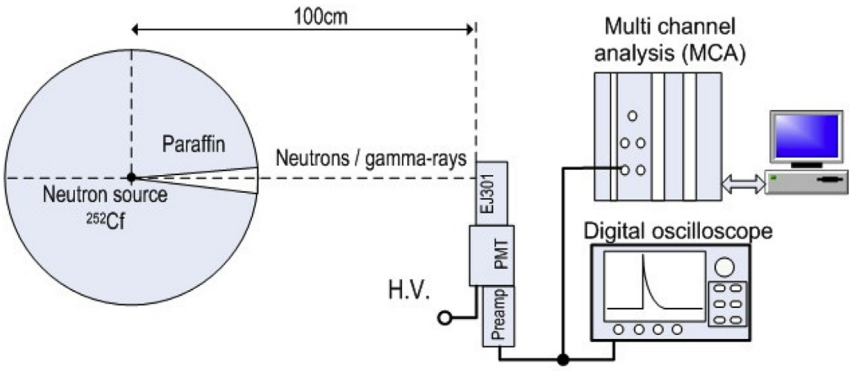

Fig. 3. Experimental arrangement.

energy of the gamma ray, electron rest mass, and speed of light in vacuum, respectively. The result is shown in Fig. 8, that is relation between Compton edge of gamma-ray and channel position.

Efficiency: the efficiency of the scintillation is defined as the ratio of the number of detected neutron-induced interactions divided by the number of incident neutrons. The absolute efficiency can be determined experimentally from knowledge of standard neutron field. In this work described here, the efficiency of detector was measured with ^{252}Cf neutron source (5.10^7 ± 8% Bq 5/2011). The gamma-ray effect to result was eliminated by efficiency measurement with gamma-ray sources as ^{22}Na (333 kBq 12/2000), ^{137}Cs(407 kBq 05/2011) and ^{60}Co (407 kBq 12/2000). The experimental configuration is shown as in Fig. 3; it includes a Canberra Multiport II MCA and Genie 2000 data acquisition software. The PSD methods are not included in Multiport II MCA and Genie 2000; therefore, the background spectra and ratio factor which was attracted in experiment of distinction neutron-gamma. The determined efficiency values are shown in Table 2.

Neutron gamma-ray discrimination with four PSD methods: the neutron-gamma discrimination ability of detector which includes full accessories, that was assessed by four PSD methods. The experimental configuration is shown as in Fig. 3. In this, detector was operated at −1200 V, the signal from detector was connected to first channel of DPO7254C oscilloscope via 3 m of high bandwidth cable. The pulse data were captured digitally with a sampling rate of 1 GSPS, bandwidth 2.5 GHz and 12-bit amplitude resolution. The detected events were stored on hard disk of oscilloscope. These data include gamma and neutron, therefore, the Matlab software was used to perform PSD methods which are TCT, PGA, CC and CPR methods.

Before neutron-gamma discrimination with TCT, PGA and CC methods, the sampled data were reduced noise and shaped by CR-RC digital component, after filter, the neutron or gamma pulse which has same amplitude, was shaped in discrete domain as shown in Fig. 4. The neutron pulses exhibit a larger decay time to the baseline, so the amplitude and gradients of neutron pulses are greater than that of gamma. In the TCT method, the PSD parameter is the time interval of RC-pulse overcomes the threshold. After shaped by RC filter (RC-pulse), the amplitude of neutron RC-pulses are higher than that of gamma-ray, so the time over threshold of neutrons is greater than that of the gamma-rays. In the PGA method, the PSD parameter is the slope of the tail of the RC-pulses. Survey results indicated that the separation is the best when the start time for calculating slope at after 50 ns from the top of the RC-pulse. In the CC method, the PSD parameter is the area of the neutron per gamma RC-pulse, these areas are calculated by the digital integration of RC-pulses from start point to zero-cross time point.

With the CPR method, the raw data are used directly, without filter, the PSD parameter is the angle between a pattern vector X that corresponds gamma/neutron pulses and the reference vector Y which corresponds only gamma pulses. Survey results indicated that the separation is the best when calculating from top of the pulse, and interval of 210 samples.

The FoM values were determined for each PSD algorithm, it evaluates the neutron gamma discrimination quality and was calculated as equation (3) [2,3,10-12].

$$FoM = \frac{S}{FWHM_n + FWHM_\gamma} \tag{3}$$

where S, $FWHM_n$ and $FWHM_\gamma$ are the separation between neutron and gamma peaks, full-width-half-maximum (FWHM) of neutron peak and FWHM of gamma peaks, respectively. The FoM values according to threshold and for each method are presented in

Table 2
The total efficiency value determined with ^{252}Cf,^{137}Cs,^{22}Na and ^{60}Co sources.

Sources	Activity (Bq)	Count rate (cps)	Total efficiency (%)
^{252}Cf	1.052×10^7	88,906 ± 7	14.8 ± 0.1
^{60}Co	47,962	1,732 ± 1	9.8 ± 0.2
^{137}Cs	94,474	3,869 ± 2	3.9 ± 0.3
^{22}Na	4,397	440 ± 1	17.8 ± 2.1
Background**	182		

Note: ** neutron source was closed.

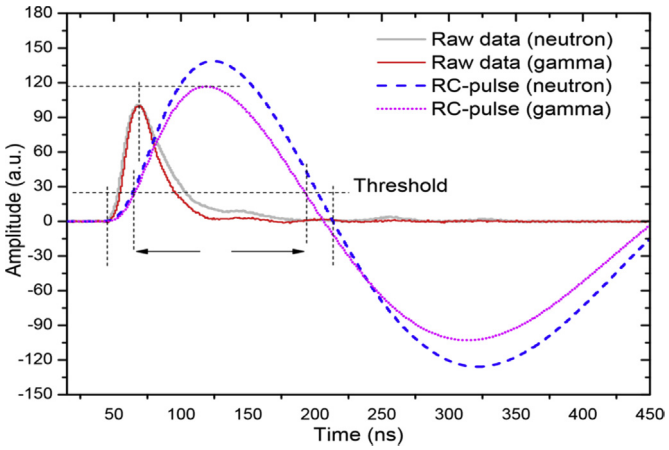

Fig. 4. Typical sample of the neutron and gamma-ray pulses with/without CR-RC shaping.

Table 3
The some values of FoM in this work and other works.

Threshold (keVee)	FoM				
	TCT	This work		CC	Other works
		PGA	CPR		
100 ÷ 400	0.94 ± 0.16	0.66 ± 0.13	1.01 ± 0.35	0.87 ± 0.34	1.22 [4], 1.52 [13], 1.43 ÷ 1.54 [23]
400 ÷ 700	1.21 ± 0.05	0.96 ± 0.04	1.50 ± 0.06	1.37 ± 0.07	1.47 [4], 2.19 [13]
700 ÷ 1000	1.30 ± 0.02	1.04 ± 0.03	1.59 ± 0.07	1.44 ± 0.02	1.6 [4], 2.21 [13]

Table 3 and Fig. 10. These results are an attempt to quantify PSDs performance by taking into account how well separated the Gaussian peaks are, in addition to how much the two distributions overlap by also looking at their FWHMs. In general, the PSD method has higher FoM, that is better.

3. Results and discussion

3.1. Testing the preamplifier

Table 1 presents the preamplifier test values which include measuring range based on the calibration energy scale of the detector, total noise, baseline and sensitivity.

The fluctuations of DC offset on preamplifier were measured in two cases: with and without varied input. For the latter case, the preamplifier input line was connected to the ground; the fluctuations measured in 10 minutes and repeated on 400 cycles are presented in Fig. 5, whereas average DC offset and standard deviation (Std) are 0.051 V and $1.96 \times 10^{-4} V$ (equivalent to ~0.277 keVee), respectively.

For the former case, fluctuations of base line to count rate input varied from 300 to 1700 counts per second (cps) are presented in Fig. 6, whereas average value of baseline is 35.8 mV.

The preamplifier linearity is shown in Fig. 7, whereas the relationship between input and output pulse amplitudes is presented. In this, the fitting line is linear function; gain and DC offset values are 17.85 times and 50 mV, respectively. Based on the goodness of fitting, the linear region is near above 0 mV to −150 mV corresponding to 0 V−2.70 V output, respectively. Although the DC offset is not able to reach zero and linear region is not high as other commercial preamplifiers, prototype preamplifier is qualified for neutron scintillation detectors.

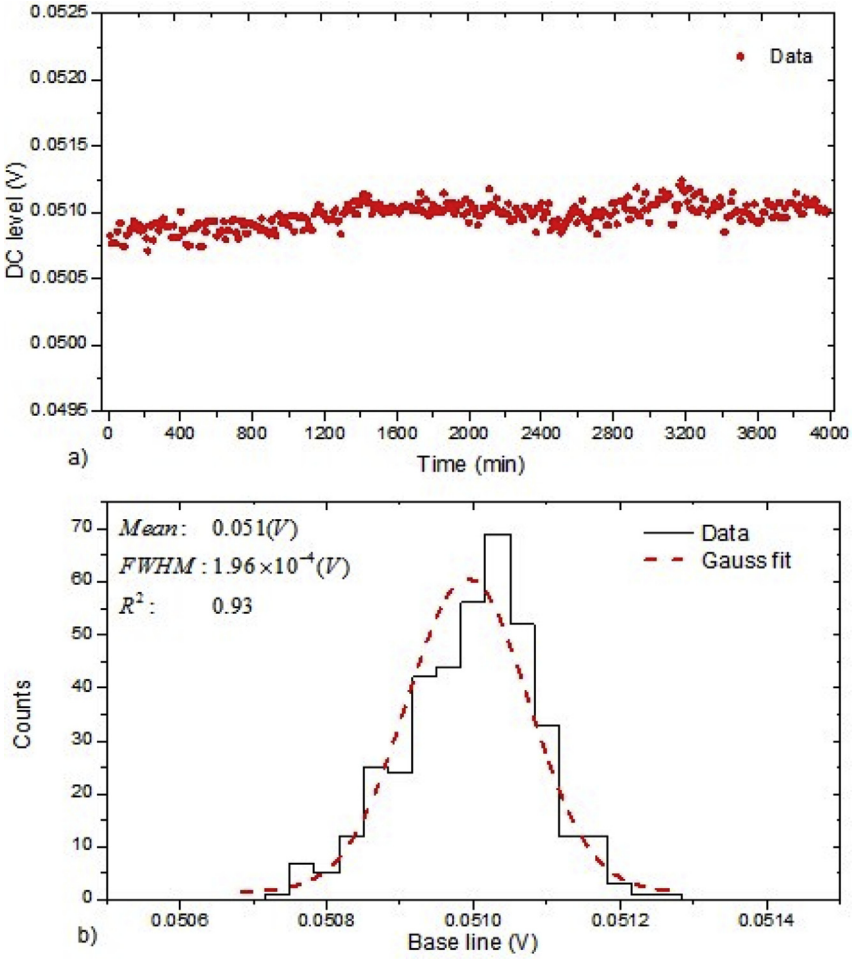

Fig. 5. The fluctuation of DC offset level of preamplifier.

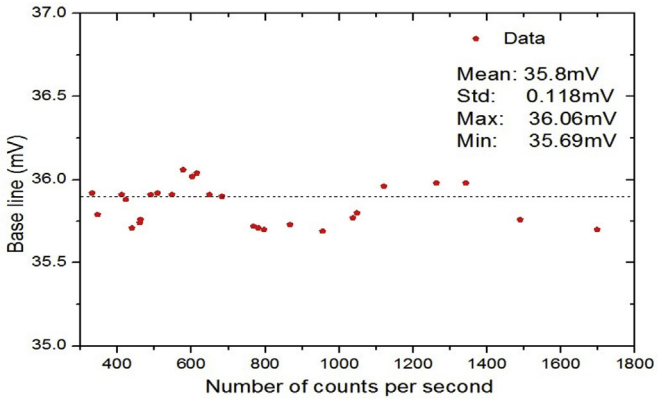

Fig. 6. The baseline values versus input count rate.

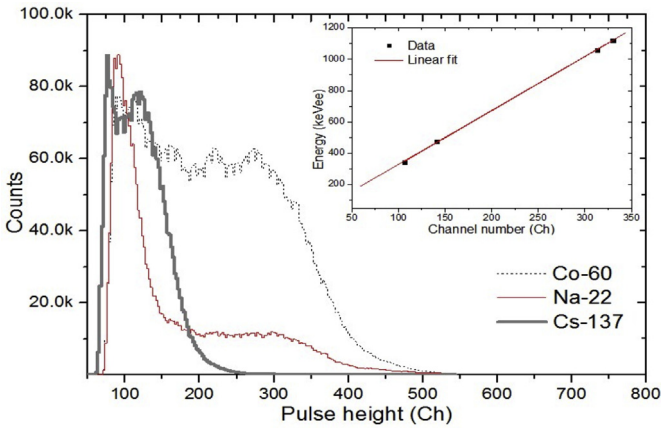

Fig. 8. The spectra of ^{60}Co, ^{22}Na and ^{137}Cs sources used for the detector's energy calibration.

3.2. Energy linearity of detector

The energy spectra of ^{60}Co, ^{22}Na and ^{137}Cs sources are shown in Fig. 8., that used the detector and oscilloscope which was operated in spectrum mode. The upper inset plot shows the line of energy calibration, in which its points are the positions of Compton edges corresponding to 511, 662, 1275 and 1332 keV photon energies that induce from radioisotope sources; and energy calibration function is E(Ch) = 3.45 × Ch - 20.4, where E and Ch are energy (keVee) and channel number, respectively.

3.3. Total efficiency

The gamma spectra presented in Fig. 8 could be seen as gamma response function of detector; these spectra agree with the results of K. Gul et al. [21] and N. A. Lurie et al. [22]. The total relative efficiency was determined based on the number of recorded events per number of events entering the detector's active volume. This result agrees with Monte Carlo calculation presented in Refs. [21,22].

3.4. Neutron-gamma discrimination and PSD methods evaluation

The specific evaluation of each PSD method is shown in Fig. 9; these are histograms of neutron and gamma ray events in which energy threshold is 300 keVee. Based on the Gaussian fit function

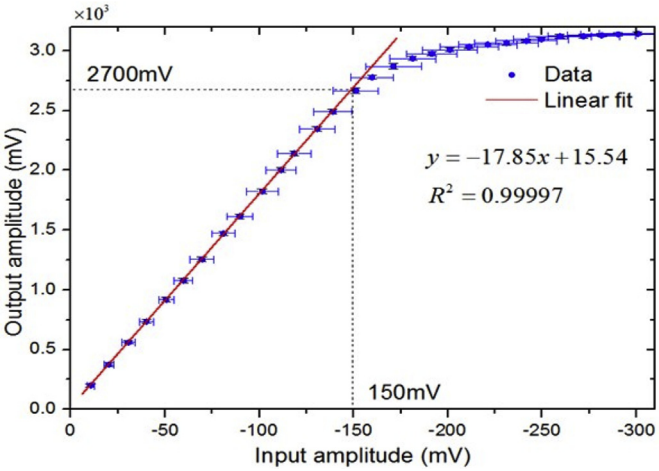

Fig. 7. The output versus input amplitude of preamplifier.

for both neutron and gamma peaks, the cutoff points which are used to separate between gamma and neutron region were found; its values for TCT, PGA, CC, and CPR methods are 159 ns, 3.01 a.u, 1469 a.u, and 0.079 rad, respectively.

The FoM values versus energy threshold are presented in Fig. 10 and Table 3.

Based on Fig. 10, the PSD capability of each method is varied to energy thresholds. At above 100 keVee threshold, the neutron/gamma discrimination of TCT, CPR and CC methods is good enough; in 100 ÷ 200 keVee region, the CPR and TCT methods have advantage; below this threshold, the TCT method is better. The neutron-gamma discrimination efficiency can be described as function of energy, that is y(x) = a*exp(-x/t) + y0; where y and x are FoM value and energy threshold, respectively; a, t and y0 are determined from fitting experimental data.

In Refs. [4,13,23], the FoM magnitude depends on energy threshold and PSD method; therefore, these FoMs agree with Refs. [4,13,23]. Based on the FoM, CPR method is better than TCT, PGA and CC methods. It is approximately 0.8 at 50 keVee and greater than 1.0 at 200 keVee threshold. The PGA method is not good as the other three methods; the FoM is less than 1.0 in the surveyed energy region. In this work, the processing time corresponding to TCT, PGA, CC and CPR methods were 260 ns, 86 ns, 170 ns and 228 ns, respectively; according to that, the PGA method is the fastest algorithm but its FoM is small.

The FoM magnitude depends on sampling resolution and FoM is larger with increasing sampling resolution. However, the CPR method is the best and agrees with Ref. [12]. The dependence of FoM on sampling resolution explained high FoM in Ref. [6]; moreover, the amplifier and shaper modules improved the signal quality, which improved capacity of ZC method at low energy threshold.

3.5. Discussion

The maximum intrinsic noise of preamplifier is equivalent to 1.13 keVee; that is very low and approximate 1% of the baseline. The output signal is linear in the range of 35.8 mV–2700 mV (0–3748 keVee); this range is not as wide as commercial fast amplifiers but satisfies for neutron measurement.

According to the efficiency and the response function presented in Table 2 and Fig. 8, this detector is not only for neutron but also gamma ray detection. Therefore, this evaluation is valuable for both neutron and gamma dose assessment.

The obtained FoM values ranging from 0.4 to 1.6 agree with

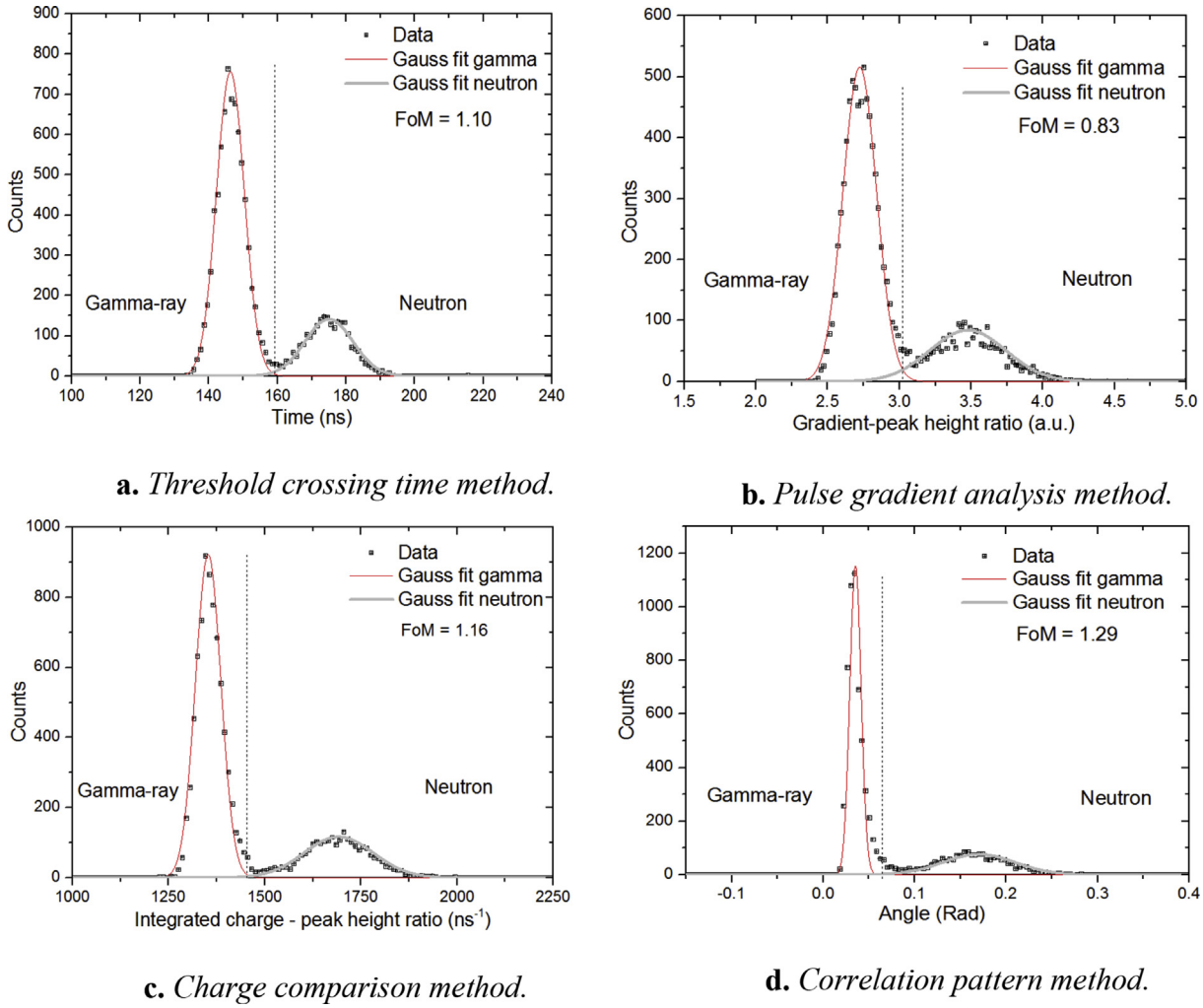

Fig. 9. The histogram of gamma and neutron events.

those of other research for NE213 detector. The detector efficiency measured with ^{252}Cf source is about 14.8% of total number of neutron entering scintillator cell, the efficiency of this detector is higher than those of the detector in Ref. [21].

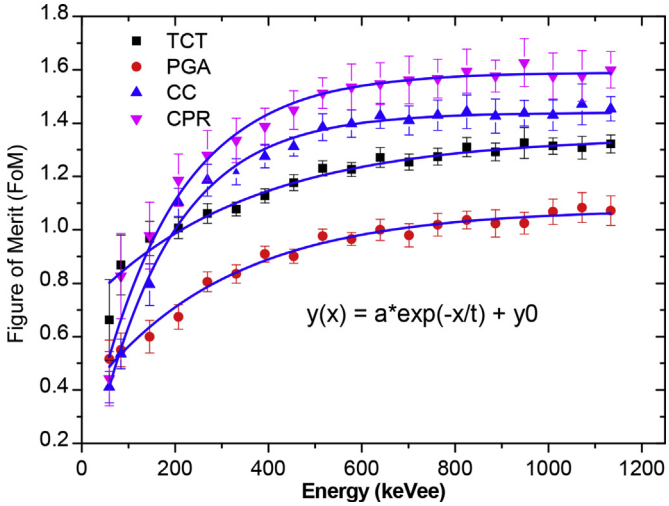

Fig. 10. The FoM values as a function of energy threshold corresponding with four methods of TCT, PGA, CC, and CPR in the range of energy from 50 to 1000 keVee.

The capacity of CPR method is the best not only at high energy but also low energy threshold. At threshold of 50 keVee, the FoM is 0.8; and up to 1.6 at higher thresholds. Over threshold of 200 keVee, the FoMs of the CC and CPR methods are similar while values of the PGA and TCT are significantly smaller. At below threshold of 200 keVee, the FoMs of the TCT method are slightly bigger than those of the CC method but they are smaller than those of the CPR method. These results are similar to the ones presented in Ref. [12], but smaller because medium active volume detector is one of the reasons to explain why the FoMs are not as big as those of small active volume detector.

At the threshold of 50 keVee, the discrimination capability between neutron and gamma of the four surveyed methods is not clear and it becomes better at the threshold of 100 keVee and increases with threshold; at threshold of 300 keVee, PSD capability of TCT, PGA, CC and CPR methods are 84.1%, 77.2%, 88.6% and 85.4%, respectively.

4. Conclusion

In this study, a compact EJ-301 scintillator neutron detector was designed and manufactured. It can be used to measure fast neutrons and separate completely neutron and gamma-rays at upper 200 keVee threshold. The equivalent energy region is linear up to

3000 keVee, corresponding to the output voltage from 35.8 mV to 2200 mV, which is compatible with the input voltage range of the high speed ADCs that can be directly inter connected.

The sensitivity of the detector achieves 707 mV/MeV while the total noise of preamplifier which contributes to signal is approximately 0.797 mV (equivalent to 1.13 keV). The average value of the baseline in the count rate range from 300 to 1700 cps is 35.8 mV and maximum variation is 0.37 mV (equivalent to 0.52 keV). With these results, the detector is reliable enough to use for neutron detection, in particular from ^{252}Cf. The CPR method presents the best neutron-gamma discrimination capacity of all.

Appendix A. Supplementary data

Supplementary data related to this article can be found at https://doi.org/10.1016/j.net.2018.07.009.

References

[1] http://www.eljentechnology.com/products/liquid-scintillators/ej-301-ej-309.pdf.
[2] B. Wan, X.Y. Zhang, L. Chen, H.L. Ge, F. Ma, H.B. Zhang, Y.Q. Ju, Y.B. Zhang, Y.Y. Li, X.W. Xu, Digital pulse shape discrimination methods for n - γ separation in an EJ-301 liquid scintillation detector, Chin. Phys. C 39 (11) (2015) 116201.
[3] G.F. Knoll, Radiation Detection and Measurement, John Wiley & Sons, 2010.
[4] C.S. Sosa, M. Flaska, S.A. Pozzi, Comparison of analog and digital pulse-shape-discrimination systems, Nucl. Instrum. Meth. A 826 (2016) 72–79.
[5] A. Rahmat, L.R. Edward, F.S. David, Development of a handheld device for simultaneous monitoring of fast neutrons and gamma rays, IEEE Trans. Nucl. Sci. 49 (4) (2002) 1909–1913.
[6] M. Nakhostin, P.M. Walker, Application of digital zero-crossing technique for neutron gamma discrimination in liquid organic scintillation detectors, Nucl. Instrum. Meth. A 621 (2010) 498–501.
[7] B.D. Mellow, M.D. Aspinall, R.O. Mackin, M.J. Joyce, A.J. Peyton, Digital discrimination of neutrons and γ-rays in liquid scintillators using pulse gradient analysis, Nucl. Instrum. Meth. A 578 (2007) 191–197.
[8] M.L. Roush, M.A. Wilson, W.F. Hornyak, Pulse shape discrimination, Nucl. Instr. Meth. 31 (1964) 112–124.
[9] G. Liu, M.J. Joyce, X. Ma, M.D. Aspinall, A digital method for the discrimination of neutrons and γ rays with organic scintillation detectors using frequency gradient analysis, IEEE Trans. Nucl. Sci. 57 (2010) 1682–1691.
[10] A. Moslem, P. Vaclav, C. Frantisek, M. Zdenek, M. Filip, Quick algorithms for real-time discrimination of neutrons and gamma rays, J. Radioanal. Nucl. Chem. 303 (2015) 583–599.
[11] M.J. Safari, D.F. Abbasi, H. Afarideh, S. Jamili, E. Bayat, Discrete fourier transform method for discrimination of digital scintillation pulses in mixed neutron-gamma fields, IEEE Trans. Nucl. Sci. 63 (1) (2016) 325–332.
[12] D. Takaku, T. Oishi, M. Baba, Development of neutron-gamma discrimination technique using pattern-recognition method with digital signal processing, Prog. Nucl. Sci. Technol 1 (2011) 210–213.
[13] E. Bayat, N. Divani-Vais, M.M. Firoozabadi, N. Ghal-Eh, A comparative study on neutron-gamma discrimination with NE213 and UGLLT scintillators using zero-crossing method, Radiat. Phys. Chem. 81 (2012) 217–220.
[14] R.A. Winyard, G.W. McBeth, Nucl. Instrum. Meth. 98 (1972) 525–533.
[15] J. Cerny, Z. Dolezal, M.P. Ivanov, E.S. Kuzmin, J. Svejda, I. Wilhelm, Study of neutron response and n-γ discrimination by charge comparison method for small liquid scintillation detector, Nucl. Instrum. Meth. A 527 (2004) 512–518.
[16] http://www.ortec-online.com/products/electronics/preamplifiers.
[17] http://www.canberra.com/products (accessed 11 September 2017).
[18] S.D. Jastaniah, P.J. Sellin, Digital pulse-shape algorithms for scintillation-based neutron detectors, IEEE Trans. Nucl. Sci. 49 (4) (2002) 1824–1828.
[19] https://www.hamamatsu.com/resources/pdf/etd/R9420TPMH1296E.pdf.
[20] IEEE Standard Test Procedures for Amplifiers and Preamplifiers Used With Detectors of Ionizing Radiation, IEEE Std 301–1988.
[21] K. Gul, A.A. Naqvi, A.H. Al-Juwair, Relative neutron detector efficiency and response function measurements with a ^{252}Cf neutron source, Nucl. Instrum. Meth. A 278 (1989) 470–476.
[22] A.N. Lurie, J.L. Harris, C.J. Young, Calculation of Gamma-Ray response matrix for 5 cm NE-213 organic liquid scintillation detector, Nucl. Instrum. Meth. 129 (1975) 543–555.
[23] A.S. Pozzi, M.M. Bourne, D.S. Clarke, Pulse shape discrimination in the plastic scintillator EJ-299-33, Nucl. Instrum. Meth. A 723 (2013) 19–23.